

THE DISCOVERY OF SEVEN EXTREMELY LOW SURFACE BRIGHTNESS GALAXIES IN THE FIELD OF THE NEARBY SPIRAL GALAXY M101

ALLISON MERRITT¹, PIETER VAN DOKKUM¹, & ROBERTO ABRAHAM²

Draft version June 11, 2014

ABSTRACT

Dwarf satellite galaxies are a key probe of dark matter and of galaxy formation on small scales and of the dark matter halo masses of their central galaxies. They have very low surface brightness, which makes it difficult to identify and study them outside of the Local Group. We used a low surface brightness-optimized telescope, the Dragonfly Telephoto Array, to search for dwarf galaxies in the field of the massive spiral galaxy M101. We identify seven large, low surface brightness objects in this field, with effective radii of 10–30 arcseconds and central surface brightnesses of $\mu_g \sim 25.5 - 27.5$ mag arcsec⁻². Given their large apparent sizes and low surface brightnesses, these objects would likely be missed by standard galaxy searches in deep fields. Assuming the galaxies are dwarf satellites of M101, their absolute magnitudes are in the range $-11.6 \lesssim M_V \lesssim -9.3$ and their effective radii are 350 pc – 1.3 kpc. Their radial surface brightness profiles are well fit by Sersic profiles with a very low Sersic index ($n \sim 0.3 - 0.7$). The properties of the sample are similar to those of well-studied dwarf galaxies in the Local Group, such as Sextans I and Phoenix. Distance measurements are required to determine whether these galaxies are in fact associated with M101 or are in its foreground or background.

Subject headings: cosmology: observations — galaxies: dwarf — galaxies: halos — galaxies: evolution

1. INTRODUCTION

In recent years, the number of known dwarf galaxies residing within the Local Group has increased dramatically (see McConnachie 2012, and references therein). The Milky Way and Andromeda (M31) galaxies are each host to dozens of faint satellites ranging in central surface brightness from 20–30 mag arcsec⁻², most of which have been uncovered in star count surveys (e.g., Ibata et al. 2007; Belokurov et al. 2010; Richardson et al. 2011; Martin et al. 2013, and several others).

Through measurements of their kinematics, Local Group satellites provide constraints on the masses of the dark matter halos of the Milky Way and M31 (e.g., Battaglia et al. 2005; Watkins, Evans, & An 2010). They also serve as testing sites for theories of cosmology and galaxy evolution on small scales. Comparisons of observed satellite abundances and internal structure with predictions from Λ CDM, for example, have led to the now familiar “missing satellite” problem (Kauffmann, White, & Guiderdoni 1993; Klypin et al. 1999; Moore et al. 1999) and the “too big to fail” problem (Boylan-Kolchin, Bullock, & Kaplinghat 2012), respectively. To more robustly determine the magnitude of the challenges faced by Λ CDM, however, we will need to expand the sample size beyond the Local Group.

Most dwarf galaxies have extremely low surface brightness. If the known Milky Way satellites were located at 5 Mpc their median integrated apparent magnitude would be $m_V \sim 21.8$, but their median central surface brightness would be $\mu_{0,V} \sim 26.1$, too faint to be detected in most integrated light surveys. Studies based on star counts are able to reach surface brightnesses of 30 mag arcsec⁻² or fainter – but only for very nearby galaxies,

as the brightness of stars, and thus the number of detectable tracer stars in a distant source, decreases with the square of the distance.³ By contrast, integrated light surface brightness is conserved with distance, and the development of integrated light techniques sensitive enough to allow dwarfs to be detected beyond the Local Group could expand the number of known dwarfs by orders of magnitude.

Several dwarf galaxies have already been identified by their low surface brightness appearance in integrated light (e.g., Karachentsev et al. 2014). Furthermore, a number of technological advances that promise to make imaging of very low surface brightness galaxies routine have recently been developed (Abraham & van Dokkum 2014). It is within this context that we describe results from a search for faint dwarf galaxies around the nearby spiral galaxy M101. We find seven previously unknown low surface brightness (LSB) galaxies, and we assess the likelihood that they are members of the M101 group.

2. DATA COLLECTION AND REDUCTION

Imaging faint galaxies in integrated light requires a telescope capable of detecting very low surface brightness emission. Our observations were taken with the Dragonfly Telephoto Array, a new robotic refracting telescope designed specifically for this purpose (Abraham & van Dokkum 2014). The telescope is comprised of an array of eight 400 mm $f/2.8$ Canon IS II telephoto lenses which, when operating together, are equivalent to an $f/1$ optical system.⁴ Nano-fabricated coatings on the optical elements of these lenses suppress internally scattered light – typically a significant obstacle to low surface brightness

¹ Department of Astronomy, Yale University, 260 Whitney Avenue, New Haven, CT, USA 06511

² Department of Astronomy and Astrophysics, University of Toronto, 50 St. George Street, Toronto, ON, Canada M5S 3H4

³ As an example, dwarfs with $M_V \sim -8$ can be detected out to ~ 1 Mpc with SDSS (Koposov et al. 2008).

⁴ This is crucial for low surface brightness imaging, as the counts per unit area on the detector decrease inversely with the square of the focal ratio f .

TABLE 1
OBSERVED PROPERTIES OF THE SAMPLE

ID	α (J2000)	δ (J2000)	g^a	$\mu_{0,g}^b$	$\mu_{e,g}^c$	$g-r$	r_e^d	n^e	b/a^f
DF_1	14 03 45.0	+53 56 40	18.9 ± 0.1	25.6 ± 0.1	26.6 ± 0.1	0.5 ± 0.2	14 ± 1	0.6 ± 0.1	0.6 ± 0.1
DF_2	14 08 37.5	+54 19 31	19.4 ± 0.2	25.8 ± 0.3	26.9 ± 0.2	0.5 ± 0.2	10 ± 1	0.7 ± 0.2	0.9 ± 0.1
DF_3	14 03 05.7	+53 36 56	17.9 ± 0.2	26.4 ± 0.2	27.4 ± 0.2	0.6 ± 0.2	30 ± 3	0.6 ± 0.1	0.7 ± 0.1
DF_4	14 07 33.4	+54 42 36	18.8 ± 0.3	26.8 ± 0.4	28.0 ± 0.2	0.6 ± 0.4	28 ± 7	0.7 ± 0.3	0.6 ± 0.1
DF_5	14 04 28.1	+55 37 00	18.0 ± 0.2	27.4 ± 0.3	28.0 ± 0.2	0.5 ± 0.4	38 ± 7	0.4 ± 0.2	0.8 ± 0.1
DF_6	14 08 19.0	+55 11 24	20.1 ± 0.4	27.5 ± 1.1	27.8 ± 0.4	0.4 ± 0.5	22 ± 8	0.3 ± 0.8	0.3 ± 0.1
DF_7	14 05 48.3	+55 07 58	20.4 ± 0.6	27.7 ± 1.6	28.7 ± 0.6	0.9 ± 0.8	20 ± 9	0.6 ± 1.0	0.5 ± 0.2

NOTE. — Structural parameters were computed using GALFIT from a stack of the g - and r -band images.

^a Integrated apparent magnitude.

^b Central surface brightness, in mag arcsec^{-2} .

^c Effective surface brightness, in mag arcsec^{-2} .

^d Effective radius, in arcseconds.

^e Sersic index.

^f Axis ratio.

imaging (Slater et al. 2009) – by an order of magnitude. The Dragonfly field of view covers $2.6^\circ \times 1.9^\circ$ in a single frame, and $3.3^\circ \times 2.8^\circ$ once dithered frames have been combined. At an assumed distance to M101 of 7 Mpc (Shappee & Stanek 2011; Lee & Jang 2012), this corresponds to $\sim 403 \times 342$ kpc. For reference, the virial radius of M101 is ~ 260 kpc.⁵

Details of data acquisition and reduction are provided in van Dokkum et al. (2014); here we give only a brief description. The data were taken during May and June of 2013 for a total of 35 hours. Calibration frames were taken on each night and applied to individual images, along with an illumination correction and an additional correction for the sky gradient. Images on a given night and across different nights were combined using optimal weighting. The final data product is comprised of reduced and star-subtracted frames in the g -band and r -band. The limiting surface brightness in the final reduced images is $\mu_g \sim 29.5$ mag arcsec^{-2} and $\mu_r \sim 29.8$ mag arcsec^{-2} on scales of ~ 10 arcsec.

3. A SEARCH FOR LOW SURFACE BRIGHTNESS OBJECTS

Six of the seven LSB galaxies presented here were initially discovered in the vicinity of M101 by visual inspection. Motivated by this, we developed a simple algorithm to allow semi-automatic detections of these and similar objects in the field (see Vollmer et al. (2013) for an example of more sophisticated methods). Our algorithm recovered the six visually-identified objects, and detected one additional galaxy (DF_3). The method is described below; it utilizes the reduced g -band and r -band images as well as their star-subtracted counterparts (see van Dokkum et al. 2014).

In order to detect all objects in each image, SExtractor (Bertin & Arnouts 1996) was run three separate times, using varied convolution filters and detection thresholds, and the three SExtractor output source catalogs were subsequently combined for each frame. The first requirement for an LSB detection was that it appeared in both g and r frames, and we therefore combined catalogs for the

two filters (for reduced and star-subtracted frames separately), excluding any detections that were only found in a single filter. Objects were matched based on their positions and relative sizes. Extended LSB objects were not removed from the star-subtracted frames along with the stars, so we further required that objects were detected there as well as in the original (i.e., pre-star subtraction) frames. Finally, we imposed conservative constraints on the size ($5 \leq R \leq 50$ pixels), median count level (≤ 0.03 counts) and scatter (≤ 0.008 counts) for detections in order to optimize the search for LSB objects.

This selection reduced the number of detections that require visual inspection from $\sim 108,098$ sources in the g -band catalog to only 529. Six of these corresponded to the original sample that was found by eye, and one additional LSB object was identified. Of the remaining 522, 28% were either wings of bright stars that were not fully subtracted, or in close proximity to stars or galaxies; 19% were false positives caused by closely spaced faint stars; and the final 53% were deemed to be noise fluctuations. Deeper observations may reveal that some candidates in this latter group are galaxies as well. An important caveat here is that our search is insensitive to the smallest galaxies; the FWHM of stars in our images is ~ 6.5 arcseconds, corresponding to ~ 200 pc at the distance of M101.

To quantify how efficiently our algorithm detects LSB objects, we simulated LSBs with a range of central surface brightness and size ($30 \leq \mu_0 \leq 23$ mag arcsec^{-2} , $6 \leq r_e \leq 50$ arcsec) and placed them at random locations in our data. The algorithm was then run on these images to determine how well the simulated LSBs were recovered. We found that $\sim 70\%$ of the simulated LSBs with properties similar to those of our observed sample were detected, but detection rates drops for other combinations of size and surface brightness. We therefore interpret our seven detections as a lower limit for the number of LSBs in the field of view.

4. STRUCTURE AND BRIGHTNESS

We used GALFIT (Peng et al. 2002) to determine the structure, luminosity, and surface brightness of the galaxies. We chose a region of 200×200 pixels around each LSB and masked out any nearby stars. We first simultaneously fit the galaxy with a Sersic (1968) profile and

⁵ Using a stellar mass of $M_* \sim 5.3 \times 10^{10} M_\odot$ (van Dokkum et al. 2014) in combination with the stellar mass - halo mass relation given by Moster et al. (2010), we estimate a halo mass of $M_h \sim 2 \times 10^{12} M_\odot$, which corresponds to a virial radius of ~ 260 kpc.

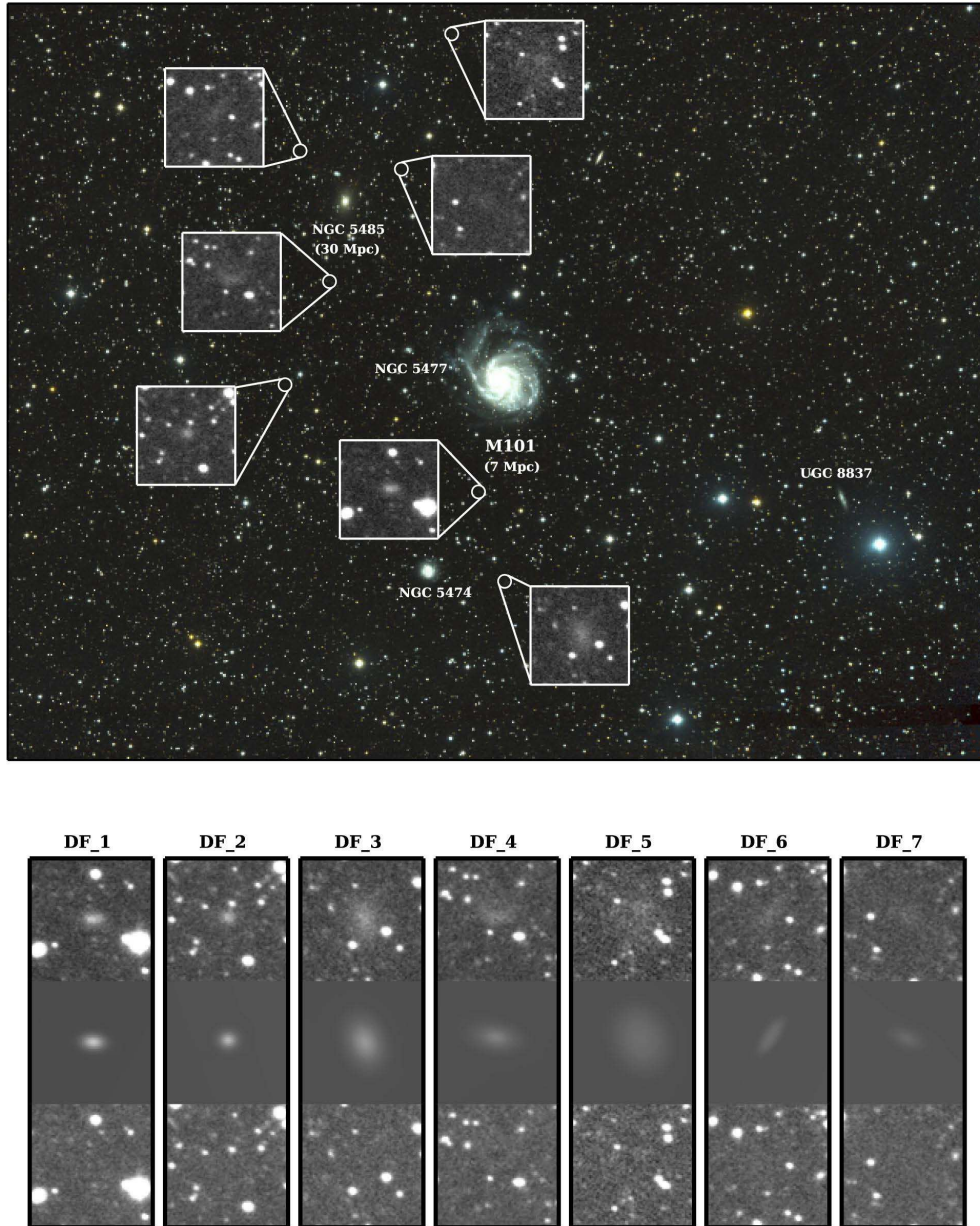


FIG. 1.— **Top:** The full $3.3^\circ \times 2.8^\circ$ Dragonfly field of view, centered on M101. The zoomed cutouts highlight the position of each of the seven newly discovered LSBs. North is up, and East is to the left. The five additional members of the M101 group that fall within our field of view (NGC 5474, NGC 5477, UGC 8837, UGC 8832) are labeled, as are the HI cloud GBT 1355+5439 and the background galaxy NGC 5485. **Bottom:** From left to right we show each of the seven LSBs. In each panel we show the central 100×100 pixels of the g -band cutouts, r -band cutouts, g -band GALFIT fits, and associated g -band residuals.

any overlapping stars with delta functions. Both the Sérsic models and delta functions were convolved with the Dragonfly PSF. A model was produced for the stars, and they were subsequently removed from the foreground of the images. Next, we stacked the g -band and r -band star-subtracted cutouts, and ran GALFIT a second time to measure the structure and orientation of the galaxies at higher S/N. Finally, we fit the luminosity and surface brightness of the galaxies in g -band and r -band individually, holding all other parameters fixed at their previously determined values. Figure 1 shows the cutouts, best fit model, and associated residuals for DF_1 - DF_7, and Table 1 contains the values for each parameter.

We find that the measured surface brightnesses of the

LSBs are low, ranging in central surface brightness from $\sim 25.5 - 27.5$ mag arcsec $^{-2}$ in g -band with corresponding surface brightnesses of $26.5 - 28.5$ mag arcsec $^{-2}$ measured at the effective radius. Effective radii range from 10 - 30 arcseconds.

The dominant source of error in our measurements of these parameters is the low signal-to-noise ratio in the fitting regions. To quantify this, we placed our best fit model of each LSB in 100 relatively empty, random locations in the M101 field. Each time, we re-measured every parameter, applying the same steps that were used for the original sample. The scatter in the values for each parameter represents the uncertainty in the fit due to noise and systematic errors such as background estima-

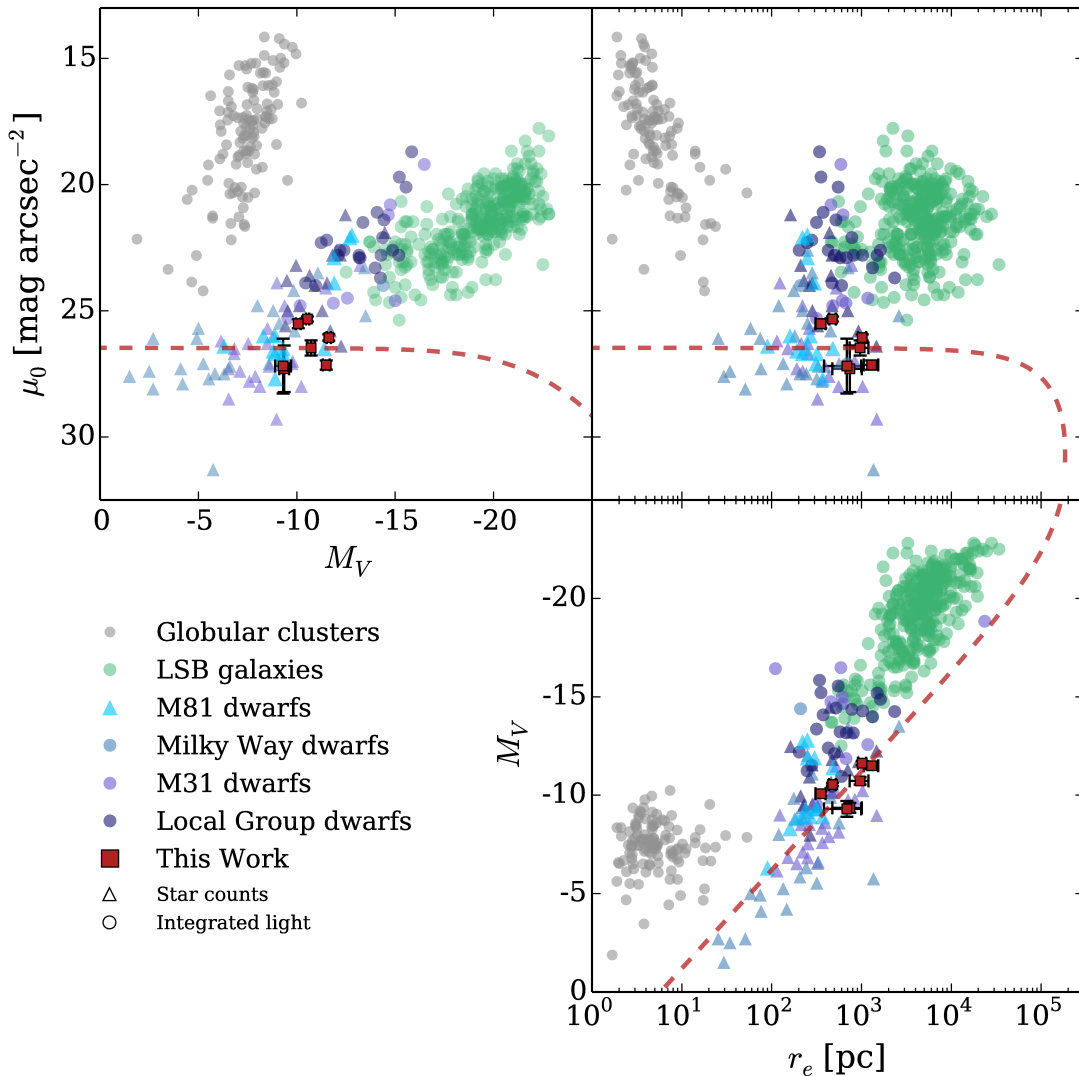


FIG. 2.— Comparison of the range in surface brightness, absolute V magnitude and effective radius of our LSB sample with that of the Local Group dwarfs (as compiled by McConnell 2012, see also references therein), nearby field LSBs (Impey et al. 1996), M81 dwarfs (Chiboucas et al. 2013) and galactic globular clusters (Harris 1996). The V magnitudes of the M81 dwarfs were converted from r -band using the conversions of Fukugita et al. 1996 and the $\langle B - V \rangle$ color of the Local Group dwarfs, and we assume $\langle B - V \rangle \sim 0.43$ (Romanishin et al. 1983) for the field LSBs. We use a distance of 7 Mpc - the red dashed line indicates where the median properties of our sample would fall for distances from the edge of the Milky Way halo out to $z \sim 2$ (including the effects of cosmological dimming).

tion. The errors are listed in Table 1.

We note that these galaxies are not detected in the Sloan Digital Sky Survey (Abazajian et al. 2009), although the central regions of the brightest few are visible in SDSS images.

5. A NEW POPULATION OF FAINT DWARFS IN THE M101 GROUP?

Given their location relative to M101 (all seven lie within its projected virial radius), we consider the possibility that these seven new LSB galaxies are dwarf satellite galaxies. In the absence of available distance measurements for the LSBs, we use comparisons of their physical properties (computed at a distance of 7 Mpc)

with those of known Local Group dwarf satellite galaxies. If the LSBs are satellites of M101, we may expect that the properties of the two populations will be consistent with one another.

In Figure 2, we plot central surface brightness as a function of effective radius and absolute magnitude for our sample and the Local Group dwarfs.⁶ The LSBs presented here have a median central surface brightness of $\mu_{0,V} \sim 26.5$ mag arcsec⁻², which is very close to the median values for the MW and M31 dwarf satellites (26.6

⁶ We converted our magnitudes from g to V using the transformations given in Fukugita et al. (1996).

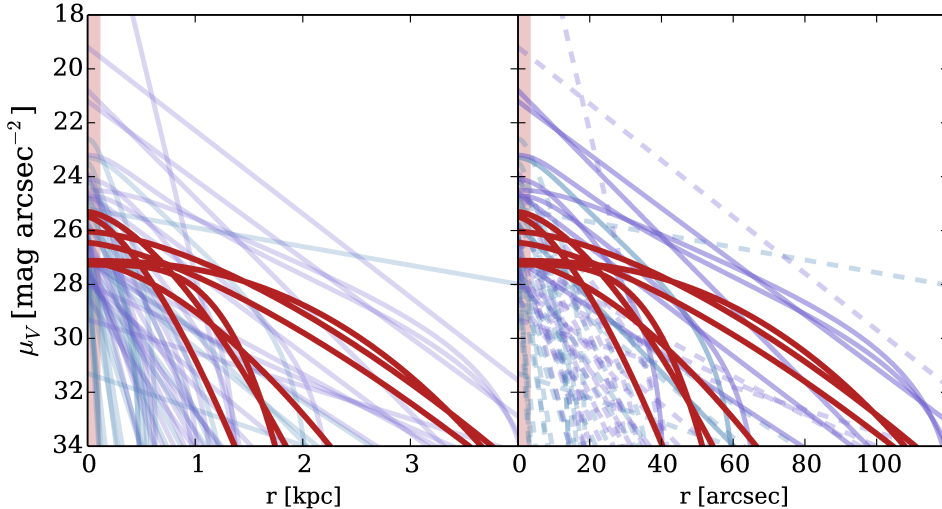


FIG. 3.— Radial profiles of the seven LSBs (red), constructed from the Sersic parameters measured by GALFIT. Blue and purple lines represent the profiles of dwarf satellites of the Milky Way and M31, respectively, and the shaded region corresponds to FWHM/2 for our data. **Left:** the physical properties of the Local Group satellites as well as those of our sample for a distance of 7 Mpc. **Right:** the *observed* properties of our sample and the implied observed properties if the Local Group satellites were at 7 Mpc. Dashed lines indicate redshifted Local Group dwarfs which, when modeled with GALFIT and placed into our data, were not detected by our algorithm.

and $26.3 \text{ mag arcsec}^{-2}$, respectively). The median absolute magnitude $M_V \sim -10.5$ is also typical of the Local Group dwarfs. Furthermore, we find that the integrated colors are similar: the median color of the LSB sample is $\langle g - r \rangle \sim 0.5$, or $\langle B - V \rangle \sim 0.7$, whereas the brighter Local Group dwarfs (which have M_V comparable to our sample) have a median color of $\langle B - V \rangle \sim 0.63$ (Mateo 1998, and references therein). The sizes of the LSBs span a range that is very similar to that of the M31 satellites, but are consistent with only the largest of the known Milky Way satellites. As noted previously, we cannot detect the smallest satellites due to the 6.5 arcsecond resolution of Dragonfly.

Finally, we compare the internal structure of the galaxies. Every galaxy in our sample has a Sersic index of $n < 1$; the median value is $n \sim 0.6$. Dwarf satellites in the Local Group are typically fit with either an $n = 1$ profile (e.g., Ibata et al. 2007; Richardson et al. 2011) or with a King profile (e.g., Irwin & Hatzidimitriou 1995; de Jong et al. 2008) — the latter are similar to $n < 1$ Sersic profiles, as both have a deficit of light at the center and in the outskirts relative to an exponential profile. This is borne out in Figure 3, where we show the radial surface brightness profiles of our LSBs and of the Local Group dwarfs (using structure as reported by McConnachie 2012). In the left panel, we show the profiles of our LSBs (at 7 Mpc) alongside the profiles of the Local Group dwarfs, and in the right panel we show the observed profiles of the LSBs with redshifted profiles of the Local Group dwarfs. The light profiles of the LSBs and the Local group dwarfs encompass a range of properties, but are consistent with one another.

6. DISCUSSION

In this *Letter* we have presented the discovery of seven LSB galaxies in the field of the nearby spiral galaxy M101. The galaxies in our sample range from $25.5 - 27.5 \text{ mag arcsec}^{-2}$ in central surface brightness and have Sersic indices $n < 1$. As shown in Figures 2 and 3, the prop-

erties of the LSBs are similar to those of dwarf satellites in the Local Group, but we stress that without distance measurements for these galaxies other interpretations are possible. Here we provide a discussion of the implications of associating the LSBs with M101 and also explore some additional scenarios.

To date, the M101 group is known to consist of seven relatively bright companions ($-19 < M_V < -14$; Giuricin et al. (2000); Karachentsev et al. 2014), five of which fall within our field of view. Additionally, Mihos et al. (2012) discovered two HI clouds in the vicinity of M101 - one, GBT 1355+5439, lies in our field, but we do not detect any signal above the limiting surface brightness (see Section 2) at that location. In Figure 4 we show the cumulative luminosity function (CLF) for the M101 group with the LSBs included, along with the observed CLFs of the Milky Way and M31 for comparison. We note that for $M_V \lesssim -9$, the M101 group CLF is remarkably similar to that of M31. Another point of interest is the apparent arrangement of the LSB galaxies - all seven were discovered to the east of M101. Particularly in the context of the lack of observed tidal streams or stellar halo down to $\gtrsim 30 \text{ mag arcsec}^{-2}$ (Mihos et al. 2013; van Dokkum et al. 2014), this may indicate that the galaxies are part of an infalling low mass group (e.g., Tully et al. 2006; Wetzel et al. 2013).

We also consider the possibility that the galaxies in this sample are not associated with M101. Measured central surface brightnesses for field LSBs out to $z \sim 0.1$ (green points, Impey et al. 1996) are shown in Figure 2, along with absolute magnitude and effective radius. It is evident from these plots that the LSBs presented here have lower surface brightness, and implied lower luminosity and smaller sizes (at 7 Mpc) than the majority of that population. The dashed red line in Figure 2 shows how these properties change as a function of distance. At large distances, our sample of LSBs would be considerably fainter than the main LSB population at fixed M_V . The interpretation of this discrepancy is not

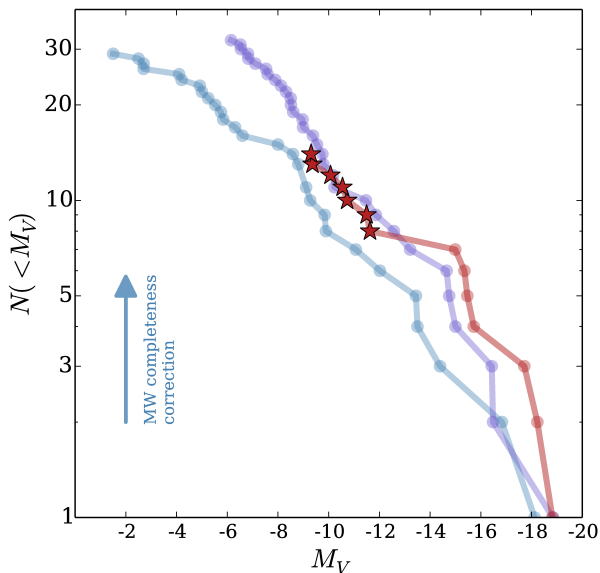


FIG. 4.— The observed cumulative luminosity function of the M101 group (red), including the LSBs presented here. We compare this to the observed CLFs of the Milky Way (blue) and M31 (purple), using data from McConnachie (2012). The arrow represents the factor of ~ 3 completeness correction for the Milky Way CLF.

straightforward, however, as the limiting surface brightness of the Impey et al. (1996) catalog is 26 B mag arcsec $^{-2}$. We therefore cannot rule out the possibility that a significant population of large, very low surface brightness field galaxies at intermediate redshift has gone undetected thus far. However, their $n < 1$ structure would be very different from known field LSBs, which often have both an exponential disk and a bulge component (e.g., Romanishin et al. 1983). Several of the galaxies are projected near the background galaxy NGC 5485 (indicated in Figure 1, located at a distance of 30 Mpc). If these galaxies are satellites of NGC 5485, their median absolute magnitude and effective radius would be $M_V \sim -13.7$ and $r_e \sim 3$ kpc. While it is plausible that

a subset of the LSBs belong to this group, their $n < 1$ profiles make this scenario unlikely. It is also possible that the LSBs reside within the halo of the Milky way – if this is the case, they would have median sizes of ~ 16 pc and luminosities of $M_V \sim -2.2$.

Given the faint, diffuse nature of the LSBs, we also assess the likelihood that we are observing galactic cirrus, planetary nebulae, or globular clusters. Optical studies have identified galactic cirrus on scales from degrees down to ~ 10 arcseconds (Guhathakurta & Tyson 1989). This range encompasses the sizes of the LSBs; however, the morphologies of the LSBs are inconsistent with the wispy and stratified nature of cirrus clouds, with the possible exception of DF_4. Planetary nebulae (PNe) have apparent magnitudes that are consistent with our LSB sample (Mal’Kov 1997); however, PNe are extremely blue in $g - r$ due to the presence of [OIII] $\lambda 4959, 5007$ in the g -band (e.g., Kniazev et al. 2014). We include a sample of globular clusters (grey points, Harris 1996) in Figure 2, and note that their properties are inconsistent with both the LSBs and the Local Group dwarfs.

The characterization of these seven new LSBs relies heavily upon determining the distance to each individual galaxy. Distance measurements for these galaxies will be difficult to obtain due to their low surface brightnesses, but may be possible with a combination of spectroscopy and high resolution imaging.

The M101 field was the first in an ongoing photometric survey of nearby galaxies with the Dragonfly telescope, and we will extend this work to searches for dwarfs around other galaxies. The discovery of LSB satellite populations around a larger sample of parent galaxies would not only provide key constraints on cosmology and galaxy evolution on small scales, but also open up the possibility of measurements of dark matter halo masses for individual galaxies (e.g., Zaritsky & White 1994; Battaglia et al. 2005).

We thank the referee for helpful comments, and the staff at New Mexico Skies Observatory for their support throughout this project. Support from NSF grant AST-1312376 and NSERC is gratefully acknowledged.

REFERENCES

- Abraham, R. G., & van Dokkum, P. G. 2014, *PASP*, 126, 55
 Abazajian, K. N., Adelman-McCarthy, J. K., Agüeros, M. A., et al. 2009, *The Astrophysical Journal Supplement Series*, 182, 543
 Battaglia, G., Helmi, A., Morrison, H., et al. 2005, *Monthly Notices of the Royal Astronomical Society*, 364, 433
 Belokurov, V., Walker, M. G., Evans, N. W., et al. 2010, *The Astrophysical Journal Letters*, 712, L103
 Bertin, E., & Arnouts, S. 1996, *A&AS*, 117, 393
 Boylan-Kolchin, M., Bullock, J. S., & Kaplinghat, M. 2012, *Monthly Notices of the Royal Astronomical Society*, 422, 1203
 Chiboucas, K. and Jacobs, B. A. and Tully, R. B. and Karachentsev, I. D. 2013, *The Astronomical Journal*, 146, 126
 de Jong, J. T. A., Harris, J., Coleman, M. G., et al. 2008, *The Astrophysical Journal*, 680, 1112
 Fukugita, M., Ichikawa, T., Gunn, J. E., et al. 1996, *The Astronomical Journal*, 111, 1748
 Giuricin, G., Marinoni, C., Ceriani, L., & Pisani, A. 2000, *The Astrophysical Journal*, 543, 178
 Guhathakurta, P., & Tyson, J. A. 1989, *The Astrophysical Journal*, 346, 773
 Harris, W. E. 1996, *The Astronomical Journal*, 112, 1487
 Ibata, R., Martin, N. F., Irwin, M., et al. 2007, *The Astrophysical Journal*, 671, 1591
 Impey, C. D., Sprayberry, D., Irwin, M. J., & Bothun, G. D. 1996, *The Astrophysical Journal Supplement*, 105, 209
 Irwin, M., & Hatzidimitriou, D. 1995, *Monthly Notices of the Royal Astronomical Society*, 277, 1354
 Karachentsev, I. D., Bautzmann, D., Neyer, F., et al. 2014, *ArXiv e-prints*
 Kauffmann, G., White, S. D. M., & Guiderdoni, B. 1993, *Monthly Notices of the Royal Astronomical Society*, 264, 201
 Klypin, A., Kravtsov, A. V., Valenzuela, O., & Prada, F. 1999, *The Astrophysical Journal*, 522, 82
 Kniazev, A. Y. and Grebel, E. K. and Zucker, D. B. and Rix, H.-W. and Martínez-Delgado, D. and Snedden, S. A. 2014, *The Astrophysical Journal*, 147, 16
 Koposov, S., Belokurov, V., Evans, N. W., et al. 2008, *The Astrophysical Journal*, 686, 279
 Lee, M. G., & Jang, I. S. 2012, *The Astrophysical Journal Letters*, 760, L14
 Mal’Kov, Y. F. 1997, *Astronomy Reports*, 41, 760
 Martin, N. F., Slater, C. T., Schlafly, E. F., et al. 2013, *The Astrophysical Journal*, 772, 15
 Mateo, M. L. 1998, *Annual Review of Astronomy and Astrophysics*, 36, 435
 McConnachie, A. W. 2012, *The Astronomical Journal*, 144, 4

- Mihos, J. C., Harding, P., Spengler, C. E., Rudick, C. S., & Feldmeier, J. J. 2013, *The Astrophysical Journal*, 762, 82
- Mihos, J. C., Keating, K. M., Holley-Bockelmann, K., Pisano, D. J. & Kassim, N. E. 2013, *The Astrophysical Journal*, 761, 186
- Moore, B., Ghigna, S., Governato, F., et al. 1999, *The Astrophysical Journal Letters*, 524, L19
- Moster, B. P., Somerville, R. S., Maulbetsch, C., et al. 2010, *The Astrophysical Journal*, 710, 903
- Peng, C. Y., Ho, L. C., Impey, C. D., & Rix, H.-W. 2002, *The Astronomical Journal*, 124, 266
- Richardson, J. C., Irwin, M. J., McConnachie, A. W., et al. 2011, *The Astrophysical Journal*, 732, 76
- Romanishin, W., Strom, K. M., & Strom, S. E. 1983, *The Astrophysical Journal Supplement Series*, 53, 105
- Sersic, J. L. 1968, *Atlas de galaxias australes*
- Shappee, B. J., & Stanek, K. Z. 2011, *The Astrophysical Journal*, 733, 124
- Slater, C. T., Harding, P., & Mihos, J. C. 2009, *Publications of the Astronomical Society of the Pacific*, 121, 1267
- Tully, R. B., Rizzi, L., Dolphin, A. E., et al. 2006, *The Astronomical Journal*, 132, 729
- van Dokkum, P. G., Abraham, R., & Merritt, A. 2014, *The Astrophysical Journal Letters*, 782, L24
- Vollmer, B., Perret, B., Petremand, M., et al. 2013, *The Astronomical Journal*, 145, 36
- Watkins, L. L., Evans, N. W., & An, J. H. 2010, *Monthly Notices of the Royal Astronomical Society*, 406, 264
- Wetzel, A. R., Tinker, J. L., Conroy, C., & van den Bosch, F. C. 2013, *Monthly Notices of the Royal Astronomical Society*, 432, 336
- Zaritsky, D., & White, S. D. M. 1994, *The Astrophysical Journal*, 435, 599